Supplementary data 1:

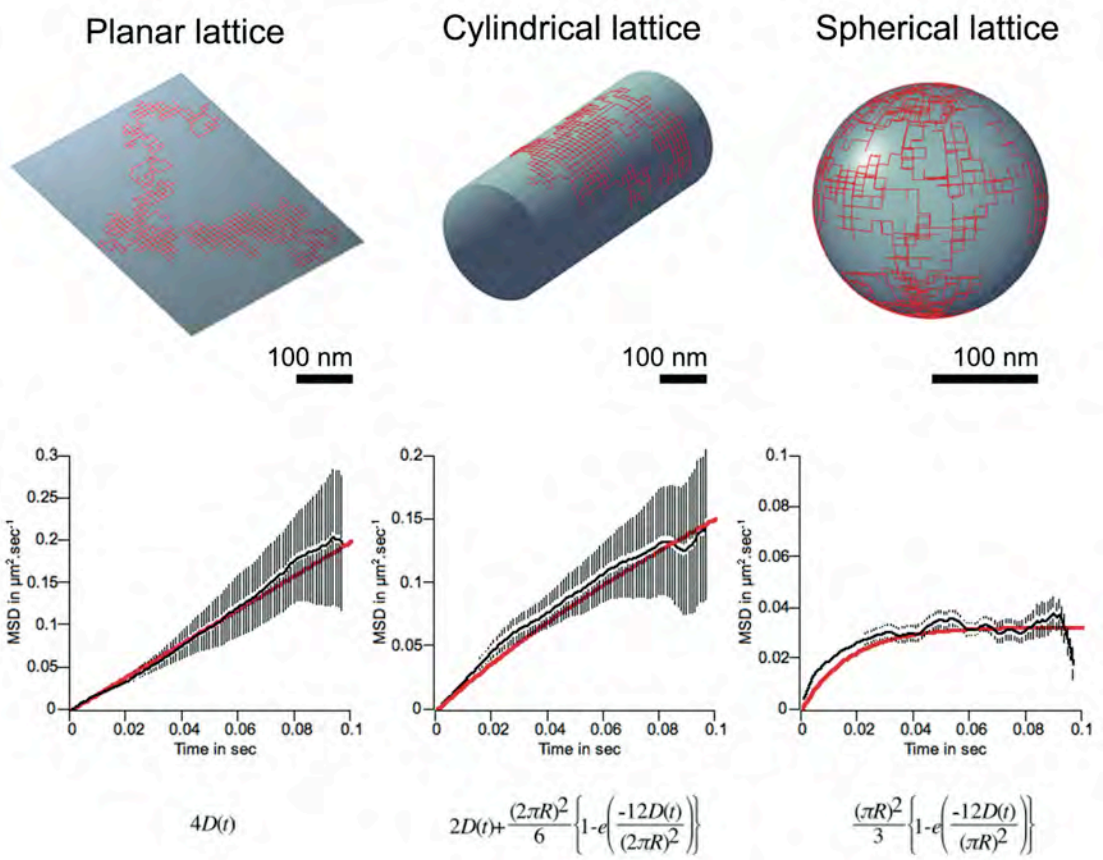

Most theoretical studies of lateral diffusion in cell membranes have considered the plasma membrane as a flat surface at the protein level. In the case of dendritic spines and other small organelles such an assumption is not valid. Thus, the precise relationship between surface topology and Brownian motion has been poorly described (1). To clarify the effect of membrane shape on lateral diffusion we computed random walks (first row in the figure, 100 ms trajectory of one particle in red) on lattices of planar, cylindrical and spherical (with radius R is 100 nm) shapes and measured the mean square displacement (MSD). The scale of the simulation was set such that the spacing between lattice sites was 10 nm (or 10/R in rad for angular displacement) and the time step was 50 μs, the microscopic diffusion coefficient was then 0.5 $\mu m^2/s$. On the planar lattice the particle randomly jumped to one of the four cardinal positions; on the cylindrical lattice two positions where located online with the starting point while the two other positions where located on a cross section circle; finally, on the spherical lattice the four possible positions per jump where located on perpendicular geodesic circles.

Mean square displacements were computed as:

$$MSD(n\delta t) = \left(N-1-n\right)^{-1} \sum_{j=1}^{N-1-n} \left\{ \left[x_{(j\delta t+n\delta t)} - x_{(j\delta tt)} \right]^2 + \left[y_{(j\delta t+n\delta t)} - y_{(j\delta t)} \right]^2 \right\}$$

(2) where δt is the time-resolution (1 ms in our experiments) and $(x(j\delta t+n\delta t), y(j\delta t+n\delta t))$ describes the particle position following a time interval $n\delta t$ after starting at position $(x(j\delta t), y(j\delta t))$; N is the total number of frames in the sequence. We used the radial distance on cylindrical lattice runs and the geodesic distance on spherical lattice runs to compute MSDs.

The bottom row on the figure shows the MSDs computed in each case for one particle during a 100 ms run (in black with SEM, corresponding fit in red). As already described, free Brownian motion on planar lattices produce MSD growing linearly with time intervals with a slope of $4D$, where D is the microscopic diffusion coefficient. On the cylindrical lattice, a semi-closed surface, the diffusion is restricted in one dimension and free in the other, hence the MSD curves have two components. The free motion component grows linearly (with a slope of $2D$) and the confined motion component growing asymptotically and approaching $L^2/6$ as described by Kusumi et al. (2) (L is the limit distance covered in one dimension, $2\pi R$ onto a cylinder). Thus, MSD curves can be fitted by:

$$MSD(t) = 2D(t) + \frac{(2\pi R)^2}{6}\left\{1 - e\left(\frac{-12D(t)}{(2\pi R)^2}\right)\right\}$$

as in Tardin at al. (3) adapted from (2), t is the time interval. This result suggests that the macroscopic diffusion coefficient on small cylindrical regions such as axons or dendritic shafts is half the microscopic diffusion coefficient. On a sphere, a closed surface, a particle ongoing a random walk is confined to the area of the sphere and thus undergo confined motion so the computed MSD grows asymptotically to approach $(\pi R)^2/3$, giving the following fit:

$$MSD(t) = \frac{(\pi R)^2}{3}\left\{1 - e\left(\frac{-12D(t)}{(\pi R)^2}\right)\right\}$$

Together, these data suggest that simple models of diffusion in non-planar surfaces can generate anomalous diffusion leading to the conclusion that membrane topology is a key regulator of protein diffusion in organelle's membrane.

Supplementary data 2:

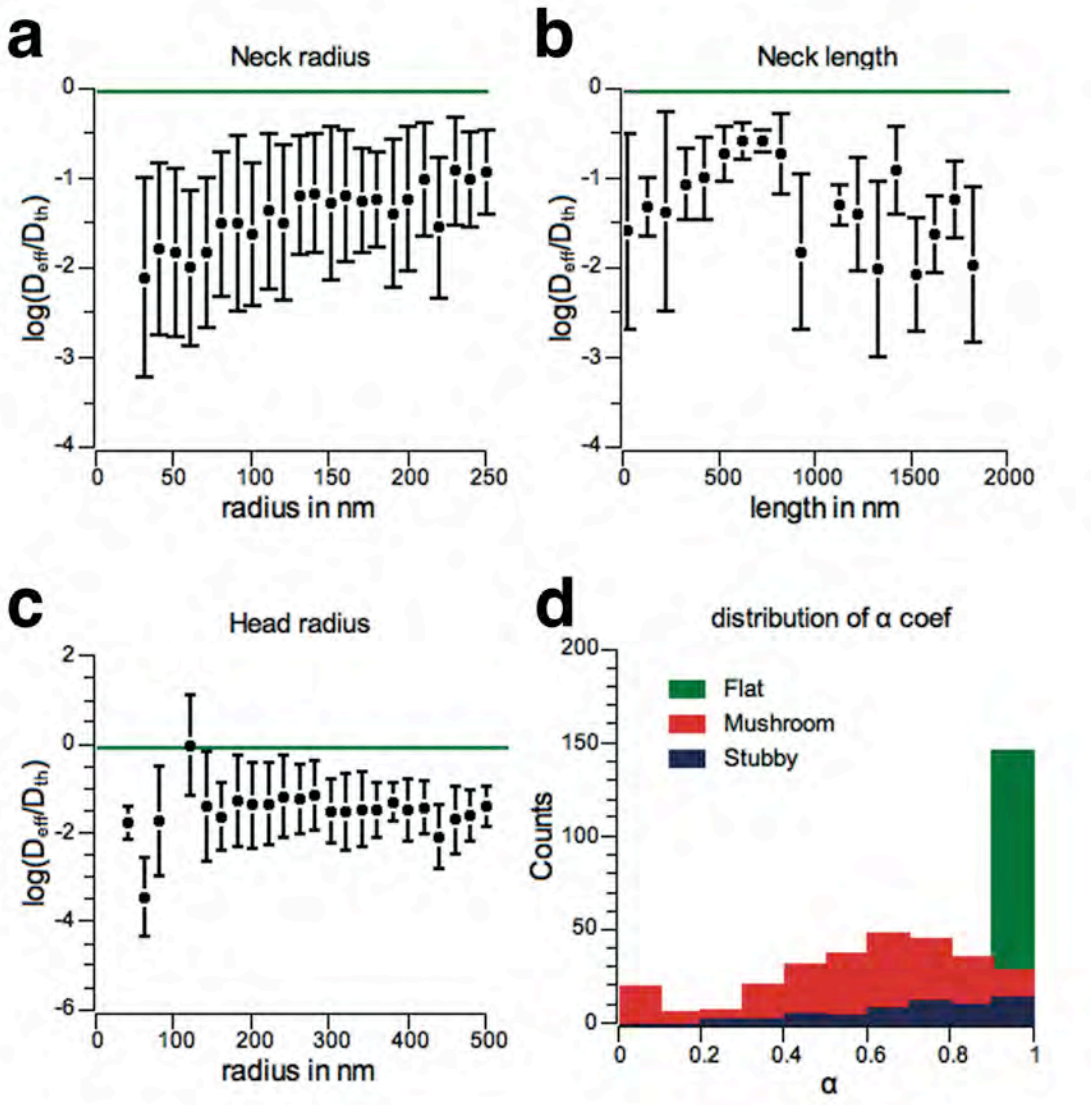

a, b and c respectively display the relationship between $\log(D_{eff}/D_{th})$ and the neck radius, neck length and head radius. No correlation was observed for any of these parameters (n=512). Data were grouped (bin sizes, 10 nm for neck radius, 100 nm for neck length and 20 nm for head radius) and mean ± sem were plotted. d represents the distribution of α, the time exponent computed in fits, for flat, stubby and mushroom spines (n=256 for flat and stubby, n=512 for mushroom). For simulations on flat membrane α is equal or close to 1 as expected for free Brownian motion. The time exponent decreases for mushroom and stubby spines consistent with the topology induced anomalous diffusion.

Supplementary data 3:

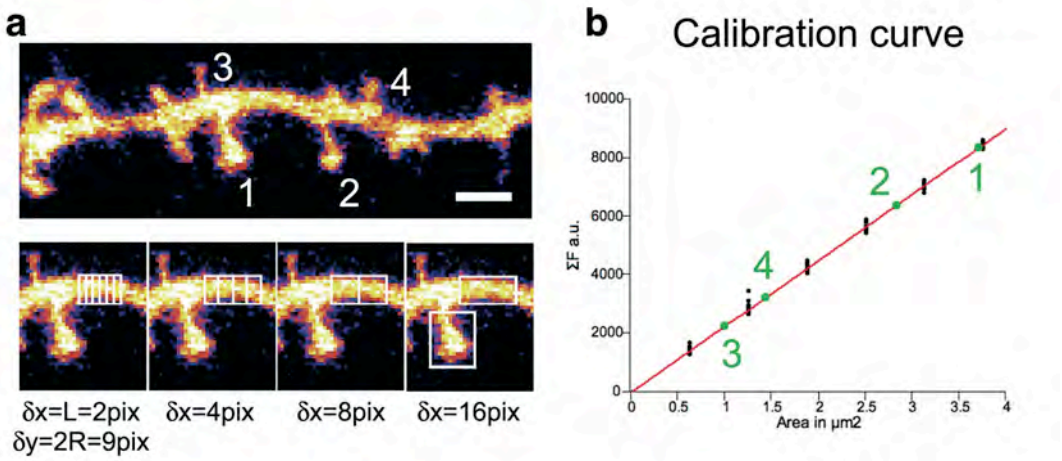

To accurately measure spine membrane area we built calibration curves with the assumption that the dendritic shaft is a cylinder. First we measured the total fluorescence emitted from various lengths of shaft (a, bottom row). Then, using the cross section as the diameter, we calculated the corresponding membrane area. From the resultant calibration curve (b) we determined spine area (1-4) from the total fluorescence. Scale bar = 1 μm.

Supplementary data 4:

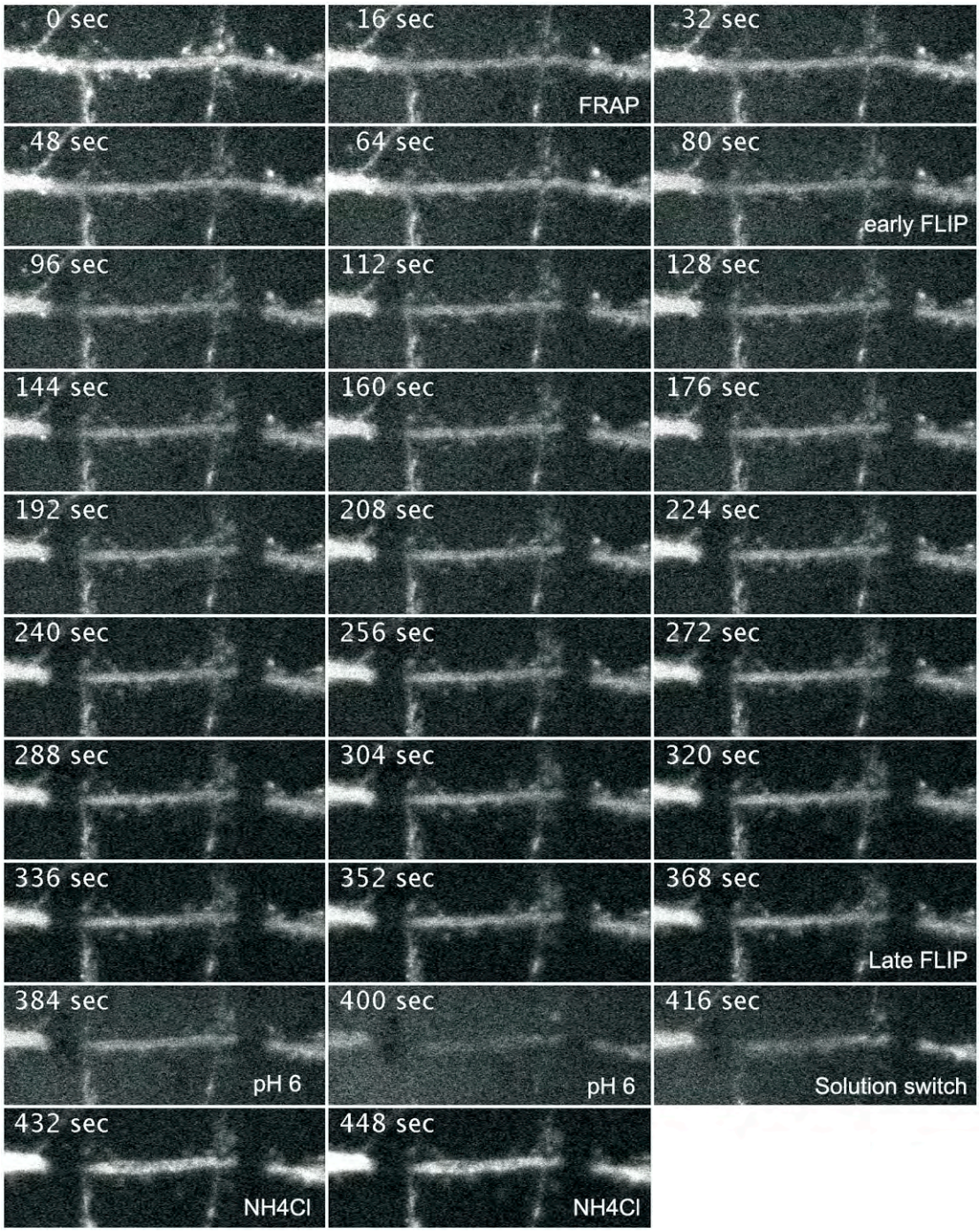

These images are example raw data for the time course shown in Figure 1b with the final panels demonstrating the effect of NH_4Cl application. As can be seen there is now dramatic increase in fluorescence in the presence of NH_4Cl indicating that there is a substantial pool of intracellular receptors in the shaft but not in spines.

Supplementary data 5:

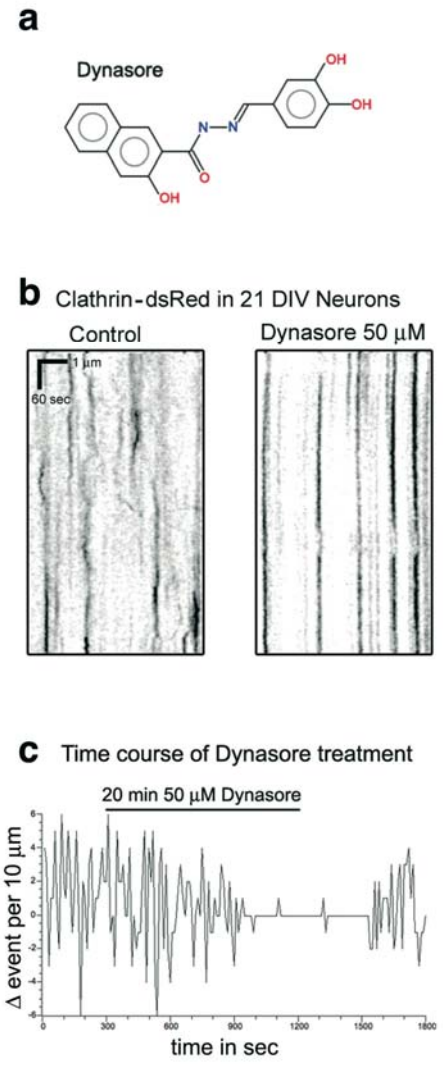

Dynasore (a) is a dynamin GTPase activity inhibitor. To validate our custom synthesized dynasore 21 DIV neurons were transfected with dsRed tagged clathrin and recorded kymographs of clathrin coated pits along a section of dendrite (b). In control conditions (1/1000 DMSO) clathrin coated pits assemble and disassemble rapidly (mean half-life is 84 sec), after 20 min Dynasore 50 µM pretreatment, clathrin coated pits were immobilized indicating that endocytosis was effectively blocked. c, Time course of dynasore application on clathrin coated pits. Dynasore activity is assessed by the variation in the number of clathrin pits in between two frames (1 frame/10 sec).

Additional bibliography:

1. Aizenbud, B. M., and Gershon, N. D. (1982) *Biophys J* 38, 287-293
2. Kusumi, A., Sako, Y., and Yamamoto, M. (1993) *Biophys J* 65, 2021-2040
3. Tardin, C., Cognet, L., Bats, C., Lounis, B., and Choquet, D. (2003) *Embo J* 22, 4656-4665